



Attenuation of MAMLD1 Expression Suppresses the Growth and Migratory Properties of Gonadotroph Pituitary Adenomas

Junhui Qi¹ · Wei Ni^{2,3}

Received: 7 December 2018 / Accepted: 8 February 2019 / Published online: 25 March 2019
© Arányi Lajos Foundation 2019

Abstract

Gonadotroph pituitary adenomas (GPA) constitute approximately 15–40% of pituitary tumors. Some GPAs can be highly infiltrative, making full surgical resection challenging and increasing the risk of recurrence. The transcriptional co-activator Mastermind-Like Domain Containing 1 (MAMLD1, CXorf6, F18) is involved in regulating signaling pathways important in pituitary tumorigenesis, including the Notch signaling pathway. However, MAMLD1's role in GPA remains unknown. GPA biopsies were collected from 96 patients following surgery, who were monitored until tumor recurrence. GPA tissue was used for immunohistochemistry. The murine GPA cell lines α T3 and L β T2 were used for in vitro experiments. Lentiviral constructs were employed for MAMLD1 knockdown (KD) and dominant negative (DN) mutant experiments. Quantitative real-time PCR (qPCR) and Western blotting of MAMLD1 and Notch2 were performed. MTT and Transwell assays were used to quantify proliferation and migration, respectively. An α T3 xenograft model was established in athymic nude mice followed by fluorescent IHC of xenograft tumors. MAMLD1 and Notch2 levels correlated positively with aggressive GPAs. Increased MAMLD1 levels correlated with shortened recurrence-free survival (RFS) in aggressive GPA patients. Moreover, MAMLD1 expression independently affected patient RFS according to multivariate Cox regression. In vitro, MAMLD1 KD in the murine GPA cell lines attenuated their proliferation and migration and Notch2 expression. Additionally, DN MAMLD1^{L210X} lowered their proliferative and migratory capacity. MAMLD1 KD suppressed tumor growth and Notch2 expression in murine xenografts. MAMLD1 may serve as a predictor of GPA patient outcome and may also be leveraged as a possible therapeutic target for aggressive GPA tumors.

Keywords Pituitary adenoma · MAMLD1 · CXorf6 · Notch

Introduction

Among cancer patients with intracranial tumors, around 10–15% are pituitary adenomas [1]. More invasive pituitary tumors are highly infiltrative and frequently penetrate into the infrasellar space and correlate with greater cellular proliferation [2, 3]. Their infiltrative nature also makes full surgical

resection of these tumors challenging, consequently leading to cancer recurrence [4, 5].

Gonadotroph pituitary adenomas (GPAs, gonadotropinomas) constitute approximately 15–40% of pituitary tumors and can be identified by elevated serum levels of prolactin as well as follicle-stimulating hormone (FSH), luteinizing hormone (LH), or their subunits [6]. Although the majority of GPAs are slow growing, non-invasive tumors, a subset (ca. 21%) exhibit a more aggressive phenotype [6, 7]. Therefore, elucidation of the molecular underpinnings of aggressive GPAs and the drivers of proliferation and migration may help identify targets for better treatment options for this clinical subset of GPAs.

Previous studies have identified the transcriptional co-activator Mastermind-Like Domain Containing 1 (MAMLD1, CXorf6, F18) [8]. Most popularly, MAMLD1 mutations have been associated with supratentorial ependymoma tumors [9, 10] as well as sexual development disorders (i.e., hypospadias [11] and gonadal dysgenesis [12]). That being said, MAMLD1

✉ Wei Ni
niweikm2018@163.com

¹ Department of Neurosurgery, The Second Hospital of Yunnan Province, Kunming, People's Republic of China

² Department of Neurosurgery, The Third Affiliated Hospital of Kunming Medical University, No. 519, Kunzhou Road, Kunming, Yunnan Province 650118, People's Republic of China

³ Department of Neurosurgery, Yunnan Cancer Hospital, Kunming, People's Republic of China

is also involved in regulating signaling pathways important in pituitary tumorigenesis [13], including the Notch signaling pathway [14, 15] and the p53 tumor suppressive pathway [3, 16]. Moreover, previous research has identified a conserved transactivating binding site upstream of the MAMLD1 coding region for the key hypothalamic-pituitary nuclear receptor steroidogenic factor-1 (SF-1, NR5A1, AD4B) in both humans and mice [8, 17]. This fact is notable, since SF-1 upregulation has been strongly linked to GPAs but has not been associated with other types of pituitary adenomas [17–19]. This combined evidence suggests that MAMLD1 may be transactivated in GPAs and may affect signaling pathways (e.g. Notch) important in GPA oncogenesis.

Although this previous evidence suggests that MAMLD1 may play a role in GPA tumorigenesis, it is not known whether MAMLD1 stimulates the growth or migration of GPA cells. To address this, we investigated MAMLD1 and Notch2 levels in GPA tumors, which we found to be correlated to certain clinical features and to patients' recurrence-free survival (RFS). We also knocked down (KD) MAMLD1 to probe its impact on GPA phenotype and Notch2 expression *in vitro*. Finally, we generated a xenograft murine model to test the influence of MAMLD1 on tumor growth *in vivo*.

Materials and Methods

Statement of Ethics for Human and Animal Studies

This study was conducted according to the Declaration of Helsinki for experiments including human subjects. For use of patient-derived GPA tumor tissue and healthy pituitary tissue, this project obtained approval by the Ethics Review Committee at the third affiliated hospital of Kunming medical university. Each patient that donated GPA or healthy tissue gave their informed consent in writing prior to their involvement in the project and their privacy was observed throughout.

For animal experiments, this project obtained approval by the Ethics Review Committee at the third affiliated hospital of Kunming medical university. All animal procedures were performed according to the recommendations detailed in "Guide for the Care and Use of Laboratory Animals" manual, published by the National Institutes of Health (NIH) (8th Ed.).

GPA Patient Population

During the period from June 2012 through February 2016, GPA biopsy samples were collected from 96 patients with GPA undergoing surgery at the third affiliated hospital of Kunming medical university and the second hospital of Yunnan province. Tumor removal was accomplished either by an endoscopic transsphenoidal procedure or craniotomy. Patient diagnosis of GPA was performed using clinical and

radiological characteristics, prolactin levels, and histological microscopic analysis, including expression of pituitary-specific positive transcription factor 1 (Pit1). Exclusionary criteria were prior radio- or chemotherapy or the presence of a non-GPA pituitary adenoma. The patient population and tumor characteristics comprised: (i) 54 females and 42 males, (ii) a median age of 38 years (range: 13 to 62 years), (iii) a median pre-surgery serum prolactin level of 16.8 ng/ml (range: 2.0 to 108.9 ng/ml), and (iv) a median tumor size of 3.00 (range: 0.09 to 47.25 cm³).

GPA Patient Follow-Up

All 96 GPA patients were monitored from the time of surgery until tumor recurrence, which was defined as the duration of recurrence-free survival (RFS). Diagnosis of GPA recurrence in patients was performed within three days using clinical characteristics, serum prolactin levels, and histological analysis. Magnetic resonance imaging (MRI) was also collected and compared to the scan collected immediately post-surgery. Tumor relapse occurred in 20 out of the 50 patients that had been diagnosed with aggressive GPA in comparison to only 6 out of the 46 patients who had received a diagnosis of non-aggressive GPA. The patient population and tumor characteristics were collected as follows: (i) sex, (ii) age, (iii) average pre-surgery serum prolactin level, (iv) tumor size and invasiveness, as well as (v) MAMLD1 levels.

Patient-Derived GPA Biopsies

GPA biopsy tissue that had been collected during surgical resection was used to construct a tissue microarray (TMA) for immunohistochemistry (IHC). Three sets of biopsy samples were used for TMA-based IHC: (i) invasive GPA tissue ($n = 50$), described as Knosp grade III and IV or Hardy-Wilson grade IV [2], (ii) non-invasive GPA tissue ($n = 46$), and (iii) healthy pituitary tissue ($n = 18$) harvested in a donation program from 10 women and 8 men, with a median age of 34 years (range: 20 to 44 years). In addition, for Western blot (WB) analysis, patient-derived GPA biopsy samples ($n = 9$) were collected during the period from January 2018 through May 2018.

Generation of TMA and IHC Analysis

The patient-derived GPA biopsy samples were fixed in formaldehyde and embedded in paraffin. The resultant blocks were sectioned on a microtome and staining was performed with hematoxylin and eosin (H&E) dye. The TMAs were generated by following a protocol outlined online (<http://genome-www.stanford.edu/TMA/>). Briefly, core biopsies ($n = 3$), measuring 2 mm in diameter, were removed from every block. A Tissue Arrayer MiniCore® machine (Alphelys, Plaisir, France) was

employed to transfer the cores to a TMA, which were sectioned (4 μm), and then randomized and de-identified. All TMA slides were generated at most one week after sectioning to preserve antigenicity.

Protein levels were assessed by IHC using antibodies against: (i) Notch2 (polyclonal, rabbit, 1:500; catalog no. ab8926, Abcam, Cambridge, MA), and (ii) MAMLD1 (polyclonal, rabbit, 1:500; catalog no. HPA003923; Sigma-Aldrich). Sectioning and staining were performed on a BOND-III Fully Automated IHC and ISH Stainer (Leica Biosystems, Wetzlar, Germany). Sections were then developed employing an automated Bond Polymer Refine Detection instrument (Leica Biosystems) and visualized using an Aperio AT2 High Volume, Digital Whole Slide Scanning instrument (Leica Biosystems). Staining was semi-quantified by counting cells that displayed immunostaining as follows: (i) 0 = negative, (ii) 1 = low, (iii) 2 = medium, and (iv) 3 = high. An H-score was then computed according to the equation = (percent cells scoring 1) + 2 x (percent cells scoring 2) + 3 x (percent cells scoring 3). The intensity of MAMLD1 was classified as: (i) weak if H-score was less than 90.5 (low expression), and (ii) strong if H-score was greater than 90.5 (high expression).

Cell Lines

The SV40 T-antigen-immortalized murine GPA cell lines αT3 and $\text{L}\beta\text{T2}$ were obtained from the Department of Reproductive Medicine at the UCSD School of Medicine (San Diego, CA) [20].

Construction of Lentiviral Constructs and Transfection

For the MAMLD1 knockdown (KD) experiments, the MAMLD1-targeting (MAMLD1-pGFP-C-shLenti) and scrambled control (SCR-pGFP-C-shLenti) short hairpin (shRNA) plasmids were procured from OriGene (Rockville, MD). For the dominant negative (DN) mutant experiments, expression plasmids for WT MAMLD1 and scrambled control (SCR) were procured from OriGene (pLenti-C-GFP, catalog no. PS100065, Rockville, MD). Using the MAMLD1 WT expression vector as the PCR-based template, the DN mutant MAMLD1^{L210X} expression vector (MAMLD1 with p.L210X; c.626delT on exon 4) was created via site-directed mutagenesis using QuickChange (Stratagene, Santa Clara, CA) and a previously-described primer (forward, 5'-CAG AAG AGC CAC TGG TTT AGA TCA TCC CCA; reverse, 5'-TGG GGT TGA TCT TTT CCA GTG GCT CTT CTG) [21]. The constructs were verified by direct sequencing.

Viruses were generated in HEK293 cells that had reached subconfluency (around 80%) by transfection with virus packaging plasmids (pVSVG, pMDL, and pREV), and either pLenti-DN-MAMLD1 or pLentiSCR, and 2 mg/mL

polyethylenimine (Polysciences, Warrington, PA). Viruses were isolated 2 days later by centrifugation of filtered culturing media (16,000 g, 2 h, 4 °C). The virus preparation was then added to $\text{L}\beta\text{T2}$ or αT3 cells that had reached subconfluency (around 80%), and viral infectivity was augmented by the addition of 8 mg/mL of polybrene (Sigma-Aldrich, St. Louis, MO). Cultures with shRNA-mediated MAMLD1 KD were labeled αT3shM1 and $\text{L}\beta\text{T2shM1}$, with matching control cells labeled αT3SCR and $\text{L}\beta\text{T2SCR}$. Cultures with DN MAMLD1^{L210X} were labeled αT3DNM1 and $\text{L}\beta\text{T2DNM1}$, with matching control cells labeled αT3SCR and $\text{L}\beta\text{T2SCR}$.

Quantitative Real-Time PCR (qPCR)

A RNeasy 96 QIAcube HT Kit (catalog no. 74171, Qiagen, Hilden, Germany) was employed to isolate total RNA from the various cell lines. A RevertAid First Strand cDNA Synthesis Kit (catalog no. K1621, Thermo Fisher Scientific, Waltham, MA) was used to synthesize cDNA. qPCR reactions were setup with Platinum™ SYBR™ Green qPCR SuperMix-UDG w/ROX (catalog no. 11744500, Thermo Fisher Scientific) and readout was achieved on an Applied Biosystems™ 7500 Fast Real-Time PCR System (Thermo Fisher Scientific). MAMLD1 mRNA transcript levels were quantified by the comparative cycle threshold (C_T) approach (also known as $2^{-\Delta\Delta C_T}$ technique) and normalized to glyceraldehyde 3-phosphate dehydrogenase (GAPDH). The primers used were as follows: (i) MAMLD1 forward, 5'-GGC CCG AAT TCG GAT GGA TGA CTG GAA AAGT; MAMLD1 reverse, 5'-GAG ATC TAG CTC ATT TGG AGA AGG, (ii) DN MAMLD1^{L210X} forward, 5'-CAG AAG AGC CAC TGG TTT AGA TCA TCC CCA; DN MAMLD1^{L210X} reverse, 5'-TGG GGT TGA TCT TTT CCA GTG GCT CTT CTG, and (iii) GAPDH forward, 5'-ACC ACA GTC CAT GCC ATC ACT; GAPDH reverse, 5'-GTC CAC CAC CCT GTT GCT GTA.

WB Analysis of MAMLD1 and Notch2

Samples were homogenized in radioimmunoprecipitation assay (RIPA) buffer (Sigma-Aldrich) supplemented with a protease and phosphatase inhibitor cocktail (Roche, Basel, Switzerland). Homogenates were clarified by centrifugation (13,000 g, 10 min, 4 °C) and the supernatant's protein content evaluated by bicinchoninic acid assay (Pierce™ BCA Protein Assay Kit, Thermo Fisher Scientific). Each well of a sodium dodecyl sulfate (SDS)-polyacrylamide gel electrophoresis (PAGE gel, 10%) was loaded with 40 μg of protein. The proteins were resolved and transferred to a polyvinylidene fluoride (PVDF) membrane, which was probed in the cold room (4 °C) with antibodies against: (i) Notch2 (polyclonal, rabbit, 1:2000; catalog no. ab8926, Abcam), (ii) MAMLD1 (polyclonal, rabbit, 1:500; catalog no. HPA003923; Sigma-

Aldrich), and (iii) GAPDH (polyclonal, rabbit, 1:8000; catalog no. SAB2100894; Sigma-Aldrich). The following day, membranes were rinsed and probed with a horseradish peroxidase (HRP)-conjugated secondary antibody (Santa Cruz Biotechnology), rinsed again, and developed with an enhanced chemiluminescence reagent, and imaged with an Amersham™ Imager 6000 (GE Healthcare, Chicago, IL). Quantification was performed by densitometry.

Assays of Cellular Proliferation and Migration

An MTT assay was used to quantify proliferation in various cell lines. The assay was performed in 96-well format, cells were seeded, incubated with antibody, and treated with MTT dye followed by a solubilization buffer [CellTiter 96® Non-Radioactive Cell Proliferation Assay (MTT), catalog no.

G4000, Promega, Madison, WI]. The colorimetric signal was recorded at 490 nm on a Spectra Rainbow Microplate Reader (Tecan).

A Transwell assay was used to assess migration in various cell lines. The assay was performed in 24-well format (BD Biosciences, San Jose, CA) with chambers possessing 8 μm pore size (Corning® Costar®, Corning, NY). Cells (10⁵ per well) were seeded within the top chamber in Matrigel™ (50 μg/mL; BD Biosciences) and serum-free Dulbecco's Modified Eagle's Medium (DMEM). Fixation of cells that had migrated across the Transwell and were adhered to the bottom membrane following an 18-h incubation was performed with paraformaldehyde (PFA, 4%). Staining was accomplished with Harris's hematoxylin and visualization at 200X magnification using phase contrast microscopy. Quantification was achieved by averaged cell counts from 5 randomized fields.

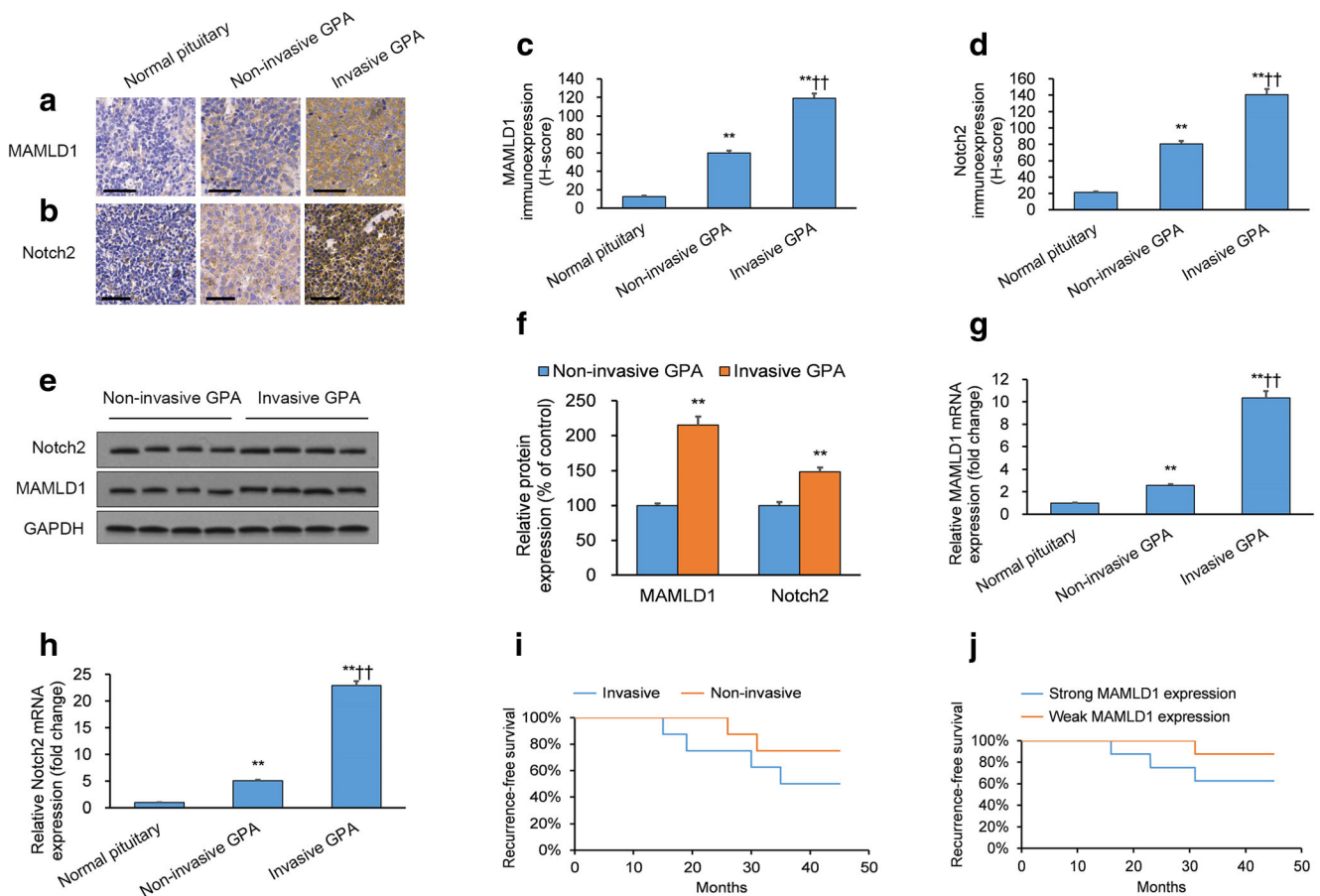


Fig. 1 Analysis of Notch2 and MAMLD1 levels in aggressive GPA and correlation with recurrence-free survival (RFS). **a, b** Typical images of tissue microarray (TMA) immunohistochemically stained for (a) MAMLD1 and (b) Notch2, which are elevated in aggressive versus non-aggressive GPAs and healthy pituitary tissue (scale bar = 60 μm). **c, d** Immunoreactivity represented in a bar graph, expressed as an H-score for (c) MAMLD1 and (d) Notch2. **p* < 0.05 and ***p* < 0.01 in comparison to healthy pituitary; †*p* < 0.05 and ††*p* < 0.01 in comparison to non-invasive GPA. **e** Typical Western blot (WB) of MAMLD1 and Notch2 in aggressive and non-aggressive GPAs with GAPDH loading

control. **f** Quantified MAMLD1 and Notch2 protein levels are greater in aggressive versus non-aggressive GPAs. **p* < 0.05 and ***p* < 0.01 in comparison to non-invasive GPA. **g, h** Quantitative real-time PCR (qPCR) quantification of mRNA transcripts for (g) MAMLD1 and (h) Notch2, which are elevated in aggressive versus non-aggressive GPAs. **p* < 0.05 and ***p* < 0.01 in comparison to healthy pituitary; †*p* < 0.05 and ††*p* < 0.01 in comparison to non-invasive GPA. **i, j** Kaplan-Meier curves of RFS for (i) aggressive GPAs and (j) high MAMLD1-expressing GPAs, which have shorter RFS durations. Bar charts display means ± SEMs

Xenograft Murine Model of α T3 Cells with/without MAMLD1 KD

Xenografts of α T3 cells with/without shRNA-mediated MAMLD1 KD were established in athymic nude mice (aged 6 weeks) that were procured from Vital River Laboratory (catalog no. SCXK2012–0001, Beijing, China). Animals were housed under aseptic conditions following standard protocols. A subcutaneous injection of α T3shM1 or α T3SCR cells (2×10^6) was made on day zero into the hind flank of each mouse ($n = 12$ mice per injected cell type). A blinded investigator used calipers to take tumor measurements [length L (mm) and width W (mm)] on every fourth day. The volume (V) was obtained by applying the equation $V (\text{mm}^3) = 0.5 \times L \times W^2$. Four weeks after the cancer cells were injected, the mice were euthanized, and their tumors reserved for additional experiments.

Fluorescent IHC of Xenograft Tumors

Mice were placed under deep anesthesia before perfusion was performed using PFA (4%). Tumors were then excised and soaked in PFA (4%) in the cold room. The next day, embedding in Tissue-Tek™ O.C.T. media (optimal cutting temperature; Sakura) was performed, followed by flash freezing (-80°C) in n-hexanes. Blocks were sectioned on a cryostat microtome (Leica Biosystems) to a thickness of $10 \mu\text{m}$. Tissue sections were rinsed in phosphate buffered saline (PBS) and then probed at 4°C with antibodies against: (i) Notch2 (polyclonal, rabbit, 1:200; catalog no. ab8926, Abcam), and (ii) MAMLD1 (polyclonal, rabbit, 1:100; catalog no. HPA003923; Sigma-Aldrich). The next day, sections were rinsed and probed for two hours at 4°C with a secondary antibody Donkey Anti-Rabbit IgG conjugated with Alexa Fluor® 488 (1:1000; catalog no. ab150073, Abcam). After additional rinse steps, sections were laid on slides and were

Table 1 Univariate and multivariate analyses for the clinicopathological correlates of recurrence/progression-free survival

Variable	Recurrence		Univariate analysis				Multivariate analysis			
	Yes	No	RR	95% CI lower bound	95% CI upper bound	P value	OR	95% CI lower bound	95% CI upper bound	P value
Gender										
Male	8	34	1.000	–	–	0.244	1.000	–	–	0.254
Female	18	36	2.0944	0.594	6.6190		2.090	0.559	7.472	
Age										
≤37	16	32	1.000	–	–	0.367	1.000	–	–	0.891
>37	10	38	1.5930		5.3448		1.144	0.347	3.471	
Tumor volume (cm^3)										
≤3.00	10	38	0.5623		1.7029	0.273	2.894	0.535	14.626	0.206
>3.00	16	32	1.000	–	–		1.000	–	–	
Preoperative serum prolactin (ng/ml)										
≤16.8	10	38	1.000	–	–	0.294	1.000	–	–	0.634
>16.8	16	32	0.5764	0.176	1.7726		0.715	0.189	2.808	
Invasiveness										
Invasive	20	30	1.000	–	–	0.060	1.000	–	–	0.301
Non-invasive	6	40	0.2796	0.076	1.0152		0.359	0.054	2.514	
MAMLD1 expression										
Strong ($n = 48$)	22	26	1.000	–	–	0.009*	1.000	–	–	0.035*
Weak ($n = 48$)	4	44	0.1407	0.030	0.5950		0.154	0.029	0.895	

* $p < 0.05$

immersed in mounting medium with DAPI (ZSGB-BIO, Beijing, China). Slides were visualized by confocal laser scanning microscopy (Leica Microsystems, Wetzlar, Germany).

Statistical Tests and Analyses

Kaplan-Meier curves (log-rank) were employed to assess the correlation between MAMLD1 and recurrence-free survival (RFS) in patients. Multivariate Cox proportional-hazards regression was utilized to investigate features of GPA tumor tissue that independently predict RFS. Every *in vitro* experiment was executed with a minimum of three replicates and the results represented by the mean \pm standard error of the mean (SEM). Student's *t* test was employed to assess variation among two

experimental conditions. Variation between three or more experimental conditions was assessed by one-way analysis of variance (one-way ANOVA). Least significant difference (LSD) test was then applied post hoc to extract *p* values.

Results

MAMLD1 and Notch2 Levels Are Elevated in Aggressive GPAs

We generated tissue microarrays (TMA) using 96 patient-derived aggressive ($n = 50$) and non-aggressive ($n = 46$) GPAs to evaluate their MAMLD1 and Notch2 protein levels

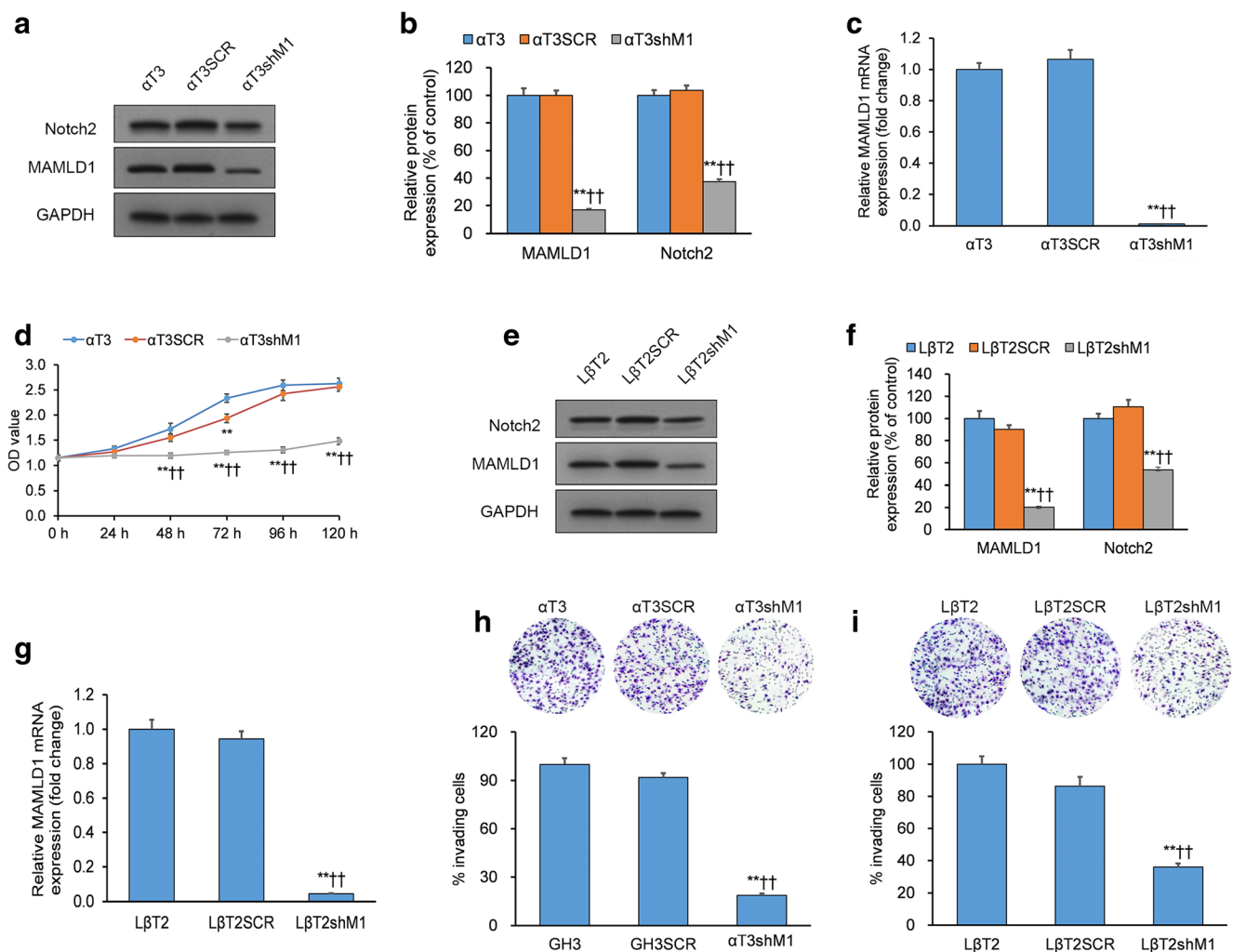


Fig. 2 MAMLD1 knockdown (KD) attenuates Notch-mediated proliferation and migration of $L\beta T2$ and $\alpha T3$ cells. **a** Typical Western blot (WB) of MAMLD1 and Notch2 in $\alpha T3shM1$ and $\alpha T3SCR$. **b** Quantified MAMLD1 and Notch2 protein levels in $\alpha T3$, $\alpha T3shM1$, and $\alpha T3SCR$. **c** qPCR quantification of MAMLD1 transcript levels in $\alpha T3$, $\alpha T3shM1$, and $\alpha T3SCR$. **d** MTT assay demonstrates that $\alpha T3shM1$ cells proliferate markedly less in comparison to $\alpha T3$ and $\alpha T3SCR$ cells. **e** Typical WB of MAMLD1 and Notch2 in $L\beta T2shM1$

and $L\beta T2SCR$ cells. **f** Quantified MAMLD1 and Notch2 protein levels in $L\beta T2$, $L\beta T2shM1$, and $L\beta T2SCR$ cells. **g** qPCR quantification of MAMLD1 transcript levels in $L\beta T2$, $L\beta T2shM1$, and $L\beta T2SCR$. **h, i** Transwell assay demonstrates that cells with MAMLD1 KD migrate markedly less in comparison to (h) $\alpha T3$ and (i) $L\beta T2$ cells. * $p < 0.05$ and ** $p < 0.01$ in comparison to $\alpha T3$ or $L\beta T2$; † $p < 0.05$ and †† $p < 0.01$ in comparison to $\alpha T3SCR$ or $L\beta T2SCR$. Bar charts display means \pm SEMs

by IHC. On average, aggressive GPAs exhibited greater MAMLD1 and Notch2 expression than did non-aggressive GPAs, and their levels correlated positively. Furthermore, elevated MAMLD1 and Notch2 protein levels were hallmarks of tumors in general, since aggressive and non-aggressive GPAs displayed enhanced expression in comparison to healthy pituitary tissue ($p < 0.05$; Fig. 1). To corroborate the IHC findings from the TMA, we examined randomly-selected aggressive and non-aggressive GPA biopsies ($n = 9$ tumors each) by Western blot (WB; Fig. 1e, f) and quantitative real-time PCR (qPCR; Fig. 1g, h), which produced the same outcome.

Higher MAMLD1 Levels Correlate with Aggressive GPAs and Recurrence-Free Survival (RFS)

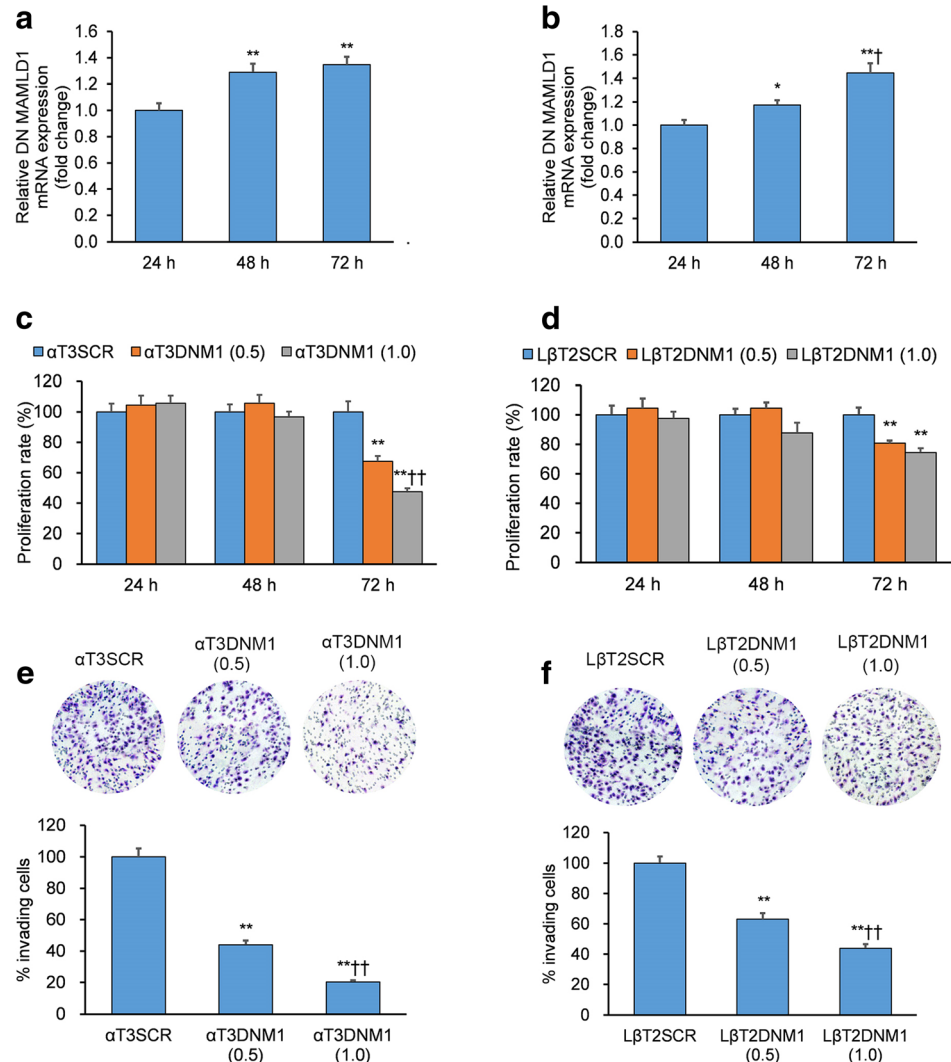
We examined the correlation of aggressive and non-aggressive GPAs with recurrence-free survival (RFS) using Kaplan-Meier log-rank test, which revealed aggressive tumors

had poorer RFS compared to non-aggressive ones (Fig. 1i). Semi-quantification by IHC using H-score classified GPA tumors as exhibiting low (H-score lesser than 90.5) or high (H-score greater than 90.5) MAMLD1 expression, which demonstrated that patients with high-expression tumors had worse RFS compared to patients with low-expression ones (Fig. 1j). Tumor MAMLD1 expression was independently prognostic of FRS according to multivariate Cox proportional-hazards regression (Table 1).

MAMLD1 Knockdown (KD) Attenuates Notch-Mediated Proliferation and Migration of α T3 and L β T2 Cells

We generated murine GPA cells (α T3 and L β T2) with shRNA-mediated knockdown (KD) of MAMLD1 (α T3shM1 and L β T2shM1, respectively) and controls with a scrambled RNA (α T3SCR and L β T2SCR, respectively). KD was verified by WB, which revealed lower MAMLD1

Fig. 3 Dominant-negative mutant inhibition of MAMLD1 attenuates proliferation and migration of L β T2 and α T3 cells. a, b Quantitative real-time PCR (qPCR) for DN MAMLD1^{L210X} mRNA expression in both (a) α T3DNM1 and (b) L β T2DNM1 cells, demonstrating that these cells' express DN MAMLD1^{L210X}. **c, d** Cellular proliferation is dose-dependently attenuated by DN MAMLD1^{L210X} (0.5 or 1.0 μ g/well) versus scrambled control (SCR) in (c) α T3 and (d) L β T2 cells. (E, F) Transwell assay quantification demonstrates that migration was dose-dependently attenuated by DN MAMLD1^{L210X} in (e) α T3 and (f) L β T2 cells. * $p < 0.05$ and ** $p < 0.01$ in comparison to SCR; † $p < 0.05$ and †† $p < 0.01$ in comparison to DN M1 (0.5). Bar charts display means \pm SEMs



levels in α T3shM1 versus α T3SCR cultures (Fig. 2a, b). Concurrently, qPCR revealed lower MAMLD1 transcripts in α T3shM1 versus α T3SCR cultures (Fig. 2c). The impact of MAMLD1 on cellular proliferation and migration were measured by an MTT and Transwell assay, respectively. α T3shM1 cells displayed both a lower proliferative (Fig. 2d) and migratory (Fig. 2h) capacity versus α T3SCR cells. Parallel experiments were performed in L β T2shM1 cells, whose MAMLD1 protein (Fig. 2e and f) and transcript (Fig. 2g) levels were decreased in comparison to L β T2SCR cells. As anticipated, L β T2shM1 cells had diminished migratory capacity in a Transwell assay than L β T2SCR cells (Fig. 2i). Since MAMLD1 has been shown to affect Notch signaling [13], we also assessed Notch2 expression levels by WB and observed that MAMLD1 KD resulted in downregulated Notch2 expression in both cell lines (Fig. 2a, b, e, and f).

Expression of MAMLD1's DN Mutant Attenuates Proliferation and Migration of α T3 and L β T2 Cells

To assess the effects of functional MAMLD1 on α T3 and L β T2 cell proliferation and migration, we generated α T3 and L β T2 cells with the non-functional DN MAMLD1^{L210X} (α T3DNM1 and L β T2DNM1, respectively) and controls with a scrambled DNA sequence (α T3SCR and L β T2SCR, respectively). We first

validated mRNA expression of the DN mutant MAMLD1^{L210X} in α T3 and L β T2 cultures and observed a steady rise over time in DN MAMLD1^{L210X} levels in both cell lines (Fig. 3a, b, respectively). Over 72 h, expression of DN MAMLD1^{L210X} lowered the viability of α T3 (Fig. 3c) and L β T2 (Fig. 3d) cells and decreased their migratory capacity as well (Fig. 3e and f).

MAMLD1 KD Attenuates Tumor Growth in Xenograft Murine Models

We generated a xenograft murine model of GPAs with/without shRNA-mediated MAMLD1 KD to examine MAMLD1's impact on GPA tumor growth in vivo by injecting nude mice with either α T3shM1 or α T3SCR cells. The tumors from α T3shM1 xenografts had a lower mean volume and final mass relative to tumors generated from α T3SCR cells (Fig. 4a–c). Fluorescent IHC analysis determined that MAMLD1 and Notch2 protein levels were lower in α T3shM1 versus α T3SCR xenograft tumors (Fig. 4d).

Discussion

Pituitary tumors exceeding 10 mm in diameter are termed macroadenomas; among these macroadenomas, approximately

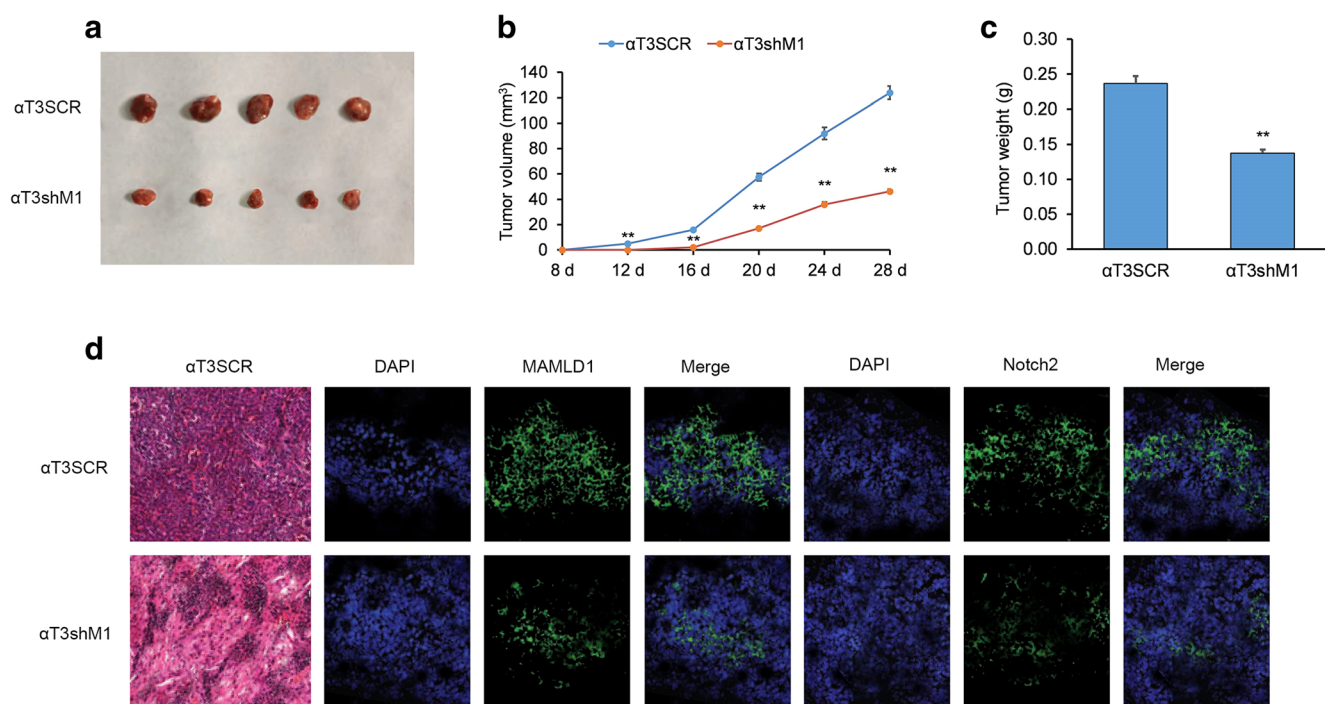


Fig. 4 MAMLD1 KD attenuates tumor growth in xenograft murine models. **a** Tumor volume was attenuated in α T3shM1 versus α T3SCR mouse xenografts. **b, c** Quantification of (b) tumor size and (c) final tumor mass of α T3shM1 and α T3SCR mouse xenografts. **d** α T3shM1 and α T3SCR tumor xenografts were stained by (top panel) hematoxylin and eosin (H&E) and (bottom panel) fluorescence immunohistochemistry

(IHC) to evaluate MAMLD1 and Notch2 protein levels. DAPI was applied as a nuclear stain. Merging images demonstrates MAMLD1 and Notch2 are markedly lower in α T3shM1 versus α T3SCR mouse xenografts (scale bar = 50 μ m). * p < 0.05 and ** p < 0.01 in comparison to α T3SCR. Bar charts display means \pm SEMs

40–50% are GPAs [6]. Clinicopathological characteristics of GPAs vary based on hormone serum levels (i.e., prolactin, FSH, LH) and on infiltration of the tumor into neighboring tissue [6]. They can be classified either as benign (ca. 79% of cases), or as aggressive, with infiltration into adjoining anatomical areas [7]. Presently, tumor removal by transsphenoidal endoscopy or transfrontal craniotomy is the best option for GPAs [7]. Unfortunately, for more aggressive cases of GPA, full surgical resection is oftentimes not possible due to widespread tumor infiltration [6]. Moreover, extensive infiltration is the most frequent reason for inadequate tumor removal [6]. In such instances of residual disease, radio- and chemotherapy are commonly necessitated as adjuvants; however, the remaining tumor may re-develop and adversely affect long-term clinical outcomes [6]. Consistent with this clinical knowledge, here we demonstrated that aggressive GPAs are associated with poorer RFS than non-aggressive GPAs according to Kaplan-Meier log-rank analysis.

MAMLD1 is a nuclear transcriptional co-activator whose expression is most pronounced in skeletal muscle, brain, and heart tissue [8, 22]. Most notably, MAMLD1 serves functions related to sexual development and homeostasis, including supporting androgen biosynthesis in the fetal testis [23], maintaining postnatal testicular growth and sperm production [24], and regulating functional luteolysis [25]. MAMLD1's sequence shows a strong, well-conserved homology to the Mastermind-Like (MAML) family of proteins by way of the MAML motif and also contains glutamine-, proline-, and serine-rich domains [8]. Although MAMLD1 is involved in regulating the Notch signaling pathway that is important in GPA oncogenesis [13–15], little is known about MAMLD1's role in GPAs. This work revealed that elevated MAMLD1 levels correlated with shorter patient RFS and that lower MAMLD1 levels independently predict RFS. We also showed that MAMLD1 stimulates GPA cell proliferation and migration using two murine GPA cell lines, which exhibited diminished proliferative and migratory capacity following MAMLD1 KD. We also found that cells with MAMLD1 KD displayed lower levels of Notch2.

From a clinical perspective, elucidation of the molecular underpinnings of aggressive GPAs and the drivers of proliferation and migration may help identify molecular targets for improved treatment options for this clinical subset of GPAs. MAMLD1, which appears to function as a Notch pathway agonist [13], was found to be increased in GPAs, suggesting these two moieties are potential therapeutic targets for GPAs. Indeed, Notch blockade is an established approach to solid tumor treatment in preclinical models [26, 27], and clinical trials are ongoing to assess the efficacy of Notch-based treatments in cancer patients [28–30]. Herein, our results bolster this approach by demonstrating that murine GPA tumor xenografts with MAMLD1 KD grow more slowly and display lower Notch2 expression relative to control xenografts.

In conclusion, we demonstrate that MAMLD1 and Notch2 are elevated in patient-derived, aggressive GPA tumors compared to non-aggressive GPAs. Furthermore, increased MAMLD1 and Notch2 expression are associated with worse patient outcomes for GPAs. We further show that MAMLD1 KD attenuates the proliferative and migratory capacity as well as the Notch2 expression of GPA cells *in vitro* and *in vivo*. Cumulatively, MAMLD1 may serve as a predictor of GPA patient outcome and may also be leveraged as a possible therapeutic target for aggressive GPA tumors.

Acknowledgements This work was supported by Medical Reserve Talent Training Project of Yunnan Province(H-2017048). The funders had no role in study design, data collection and analysis, decision to publish, or preparation of the manuscript.

Author Contributions Conceived and designed the study: Wei Ni. Performed the experimental procedures: Wei Ni and Junhui Qi. Analyzed the data: Junhui Qi. Drafted the manuscript: Wei Ni and Junhui Qi.

Compliance with Ethical Standards

Conflicts of Interest None.

References

1. Scheithauer BW, Gaffey TA, Lloyd RV, Sebo TJ, Kovacs KT, Horvath E, Yapıcıer Ö, Young WF Jr, Meyer FB, Kuroki T, Riehle DL, Laws ER Jr (2006) Pathobiology of pituitary adenomas and carcinomas. *Neurosurgery* 59(2):341–353
2. Knosp E, Steiner E, Kitz K, Matula C (1993) Pituitary adenomas with invasion of the cavernous sinus space: a magnetic resonance imaging classification compared with surgical findings. *Neurosurgery* 33(4):610–618
3. Donoho DA, Bose N, Zada G, Carmichael JD (2017) Management of aggressive growth hormone secreting pituitary adenomas. *Pituitary* 20(1):169–178
4. Dhandapani S, Singh H, Negm HM, Cohen S, Anand VK, Schwartz TH (2016) Cavernous sinus invasion in pituitary adenomas: systematic review and pooled data meta-analysis of radiologic criteria and comparison of endoscopic and microscopic surgery. *World Neurosurg* 96:36–46
5. Qian ZR, Sano T, Yoshimoto K, Asa SL, Yamada S, Mizusawa N, Kudo E (2007) Tumor-specific downregulation and methylation of the CDH13 (H-cadherin) and CDH1 (E-cadherin) genes correlate with aggressiveness of human pituitary adenomas. *Mod Pathol* 20(12):1269–1277
6. Chaidarun SS, Klibanski A, editors. *Gonadotropinomas. Seminars in reproductive medicine*; 2002: Copyright© 2002 by Thieme medical publishers, Inc., 333 Seventh Avenue, New York, NY 10001, USA. Tel:+ 1 (212) 584-4662
7. Young Jr WF, Scheithauer BW, Kovacs KT, Horvath E, Davis DH, Randall RV, editors. *Gonadotroph adenoma of the pituitary gland: a clinicopathologic analysis of 100 cases. Mayo Clin Proc*; 1996: Elsevier
8. Fukami M, Wada Y, Okada M, Kato F, Katsumata N, Baba T, Morohashi KI, Laporte J, Kitagawa M, Ogata T (2008) Mastermind-like domain-containing 1 (MAMLD1 or CXorf6) transactivates the Hes3 promoter, augments testosterone

- production, and contains the SF1 target sequence. *J Biol Chem* 283(9):5525–5532
9. Andreiuolo F, Varlet P, Tauziède-Espariat A, Jünger ST, Dörner E, Dreschmann V, Kuchelmeister K, Waha A, Haberler C, Slavc I, Corbacioglu S, Riemenschneider MJ, Leipold A, Rüdiger T, Körholz D, Acker T, Russo A, Faber J, Sommer C, Armbrust S, Rose M, Erdlenbruch B, Hans VH, Bernbeck B, Schneider D, Lorenzen J, Ebinger M, Handgretinger R, Neumann M, van Buijen M, Prinz M, Roganovic J, Jakovcevic A, Park SH, Grill J, Puget S, Messing-Jünger M, Reinhard H, Bergmann M, Hattingen E, Pietsch T (2018) Childhood supratentorial ependymomas with YAP 1-MAMLD 1 fusion: an entity with characteristic clinical, radiological, cytogenetic and histopathological features. *Brain Pathol*
 10. Archer TC, Pomeroy SL (2015) Defining the molecular landscape of ependymomas. *Cancer Cell* 27(5):613–615
 11. Chen Y, Thai HT, Lundin J, Lagerstedt-Robinson K, Zhao S, Markljung E et al (2010) Mutational study of the MAMLD1-gene in hypospadias. *Eur J Med Genet* 53(3):122–126
 12. Ruiz-Arana I-L, Hübner A, Cetingdag C, Krude H, Grüters A, Fukami M et al (2015) A novel hemizygous mutation of MAMLD1 in a patient with 46, XY complete gonadal dysgenesis. *Sex Dev* 9(2):80–85
 13. McElhinny A, Li J, Wu L (2008) Mastermind-like transcriptional co-activators: emerging roles in regulating cross talk among multiple signaling pathways. *Oncogene* 27(38):5138–5147
 14. Liu Q, Wang J, Yang H, Gao H, Li C, Lan X, Zhang Y (2018) Attenuation of EGFL7 expression inhibits growth hormone-producing pituitary adenomas growth and invasion. *Hum Gene Ther* 29:1396–1406
 15. Wang J, Liu Q, Gao H, Wan D, Li C, Li Z et al (2017) EGFL7 participates in regulating biological behavior of growth hormone-secreting pituitary adenomas via Notch2/DLL3 signaling pathway. *Tumor Biol* 39(7):1010428317706203
 16. Dong W, Zhu H, Gao H, Shi W, Zhang Y, Wang H et al Expression of cyclin E/Cdk2/p27Kip1 in growth hormone adenomas. *World Neurosurg* 2018
 17. Shinoda K, Lei H, Yoshii H, Nomura M, Nagano M, Shiba H, Sasaki H, Osawa Y, Ninomiya Y, Niwa O, Morohashi KI, Li E (1995) Developmental defects of the ventromedial hypothalamic nucleus and pituitary gonadotroph in the Ftz-F1 disrupted mice. *Dev Dyn* 204(1):22–29
 18. Asa SL, Bamberger A, Cao B, Wong M, Parker KL, Ezzat S (1996) The transcription activator steroidogenic factor-1 is preferentially expressed in the human pituitary gonadotroph. *J Clin Endocrinol Metab* 81(6):2165–2170
 19. Polidoro MA, Morace R, Arcella A, Esposito V, Giangaspero F, Jaffrain-Rea M-L, editors. Factors associated with SF1 gene expression in clinically non-functioning pituitary adenomas. 20th European Congress of Endocrinology; 2018: BioScientifica
 20. Chesnokova V, Zonis S, Zhou C, Ben-Shlomo A, Wawrowsky K, Toledano Y, Tong Y, Kovacs K, Scheithauer B, Melmed S (2011) Lineage-specific restraint of pituitary gonadotroph cell adenoma growth. *PLoS One* 6(3):e17924
 21. Camats N, Fernández-Cancio M, Audí L, Mullis PE, Moreno F, Casado IG et al (2015) Human MAMLD1 gene variations seem not sufficient to explain a 46, XY DSD phenotype. *PLoS One* 10(11):e0142831
 22. Laporte J, Kioschis P, Hu L-J, Kretz C, Carlsson B, Poustka A, Mandel JL, Dahl N (1997) Cloning and characterization of an alternatively spliced gene in proximal Xq28 deleted in two patients with intersexual genitalia and myotubular myopathy. *Genomics* 41(3):458–462
 23. Nakamura M, Fukami M, Sugawa F, Miyado M, Nonomura K, Ogata T (2011) Mamld1 knockdown reduces testosterone production and Cyp17a1 expression in mouse Leydig tumor cells. *PLoS One* 6(4):e19123
 24. Miyado M, Yoshida K, Miyado K, Katsumi M, Saito K, Nakamura S, Ogata T, Fukami M (2017) Knockout of murine Mamld1 impairs testicular growth and daily sperm production but permits Normal postnatal androgen production and fertility. *Int J Mol Sci* 18(6):1300
 25. Miyado M, Miyado K, Katsumi M, Saito K, Nakamura A, Shihara D, Ogata T, Fukami M (2015) Parturition failure in mice lacking Mamld1. *Sci Rep* 5:14705
 26. Giachino C, Boulay J-L, Ivanek R, Alvarado A, Tostado C, Lugert S, Tchorz J, Coban M, Mariani L, Bettler B, Lathia J, Frank S, Pfister S, Kool M, Taylor V (2015) A tumor suppressor function for Notch signaling in forebrain tumor subtypes. *Cancer Cell* 28(6):730–742
 27. Yuan X, Wu H, Xu H, Xiong H, Chu Q, Yu S, Wu GS, Wu K (2015) Notch signaling: an emerging therapeutic target for cancer treatment. *Cancer Lett* 369(1):20–27
 28. Aung KL, El-Khoueiry AB, Gelmon K, Tran B, Bajaj G, He B et al (2018) A multi-arm phase I dose escalating study of an oral NOTCH inhibitor BMS-986115 in patients with advanced solid tumours. *Investig New Drugs*:1–11
 29. Mir O, Azaro A, Merchan J, Chugh R, Trent J, Rodon J, Ohnmacht U, Diener JT, Smith C, Yuen E, Oakley GJ III, le Cesne A, Soria JC, Benhadji KA, Massard C (2018) Notch pathway inhibition with LY3039478 in soft tissue sarcoma and gastrointestinal stromal tumours. *Eur J Cancer* 103:88–97
 30. Massard C, Azaro A, Soria J-C, Lassen U, Le Tourneau C, Sarker D et al (2018) First-in-human study of LY3039478, an Oral Notch signaling inhibitor in advanced or metastatic cancer. *Ann Oncol* 29(9):1911–1917

Publisher's Note Springer Nature remains neutral with regard to jurisdictional claims in published maps and institutional affiliations.